Supplemental Information

Supplementary Discussion

Previous studies in mammalian cells showed that HP1, which also recognizes H3K9me3, works together with the H3K9 trimethyltransferases Su(var)3-9H1 to propagate H3K9me3 signals (Fritsch et al., 2010; Hodges and Crabtree, 2012; Nielsen et al., 2002). However, ablation of the gene encoding the H3K9me3 reader EAP-1 suppressed rather than enhanced the *spr-5(by101)* phenotypes. We speculate that EAP-1 is distinct from HP1 in that it may negatively regulate the H3K9 trimethyltransferase SET-26, either through direct interactions with SET-26, or through recruitment of the H3K9me demethylase JMJD-2 to antagonize SET-26. The mammalian homologue of EAP-1, MPP8, has been shown to interact with the H3K9me1/me2 methyltransferase GLP and the H3K9me2/me3 methyltransferase ESET (Kokura et al., 2010), consistent with the possibility that EAP-1 may accomplish the above through physical interactions with MET-2, SET-26 and/or JMJD-2. Our preliminary result suggests that EAP-1 may physically interact with JMJD2 (data not shown), consistent with such a model. Interestingly, the HP1 homologues, *hpl-1* and *hpl-2*, when knocked down, slightly accelerate the progressive sterility of *spr-5(by101)* mutant worms (Figure 5A). It will be interesting, in future studies, to determine whether these and other potential hits from our RNAi screen (Figure 5A) can further refine our molecular model of how epigenetic information is transmitted in *C. elegans*.

Supplementary Methods

Worm Strains

The N2 Bristol strain was used as the wildtype background. The following mutations were used in this study: LG1: *spr-5(by101), set-32(ok1457)*; LGII: *jmjd-2(tm2966), eap-1(ok3432), jmjd-1.1(hc184), set-13(ok2697), set-17(n5017)*; LGIII: *jmjd-4(tm965), set-25(n5021)*; LGIV: *jmjd-1.2(tm3713)*, *set-26(tm3526)*, *psr-1(tm464), set-9(n4949)*; LGV: *rde-1(ne219)*; and LGX: *jmjd-3.3(tm3197), jmjd-3.2(tm3121), set-30(gk315)*, *set-20(ok2022)*. Some of these strains have been previously used in (Andersen and Horvitz, 2007; Ashe et al., 2012; Grishok et al., 2000; Katz et al., 2009; Kleine-Kohlbrecher et al., 2010; Ni et al., 2011; Towbin et al., 2012; Whetstine et al., 2006). In this paper mutant worms were backcrossed: *jmjd-1.1:* 2-6 times, *jmjd-2(tm2966), jmjd-3.2(tm3121), jmjd-4(tm965), psr-1(tm464), set-20(ok2022), set-13(ok2697)*, and *set-25(n5021)* worms: 2 times, *set-32(ok1457)* , and *rde-1(ne219)* worms: 3 times, *jmjd-1.2(tm1373), jmjd-3.3(tm3197),* and *set-9(n4949):* 2-4 times, *set-26(tm3526):* 2-6 times, *set-17(n5017)*: 2-7 times, *set-30(gk315):* 2-8 times, and *eap-1(ok3432)*: 2-13 times.

Constructs

pGEX-4T1 was used to generate bacterial expression constructs for EAP-1, EAP-1_{chromo}, SET-17, SET-26_{SET}, and SET-30. Full length EAP-1 cDNA was amplified by PCR from wildtype cDNA using the following primers EAP-1 cDNA F ATAGGATCCATGAGTAATGAAGGTTCACGTGAAGAG and EAP-1 cDNA R TATGCGGCCGCTCAAAATTCACAACGATCGAGGAGATAC and subcloned into pGEX-4T1 between BamHI and NotI. EAP-1_{chromo} was amplified by PCR from wildtype cDNA using the following primers EAP-1_{chromo} F

ATAGGATCCCCCGAAGCAAGAGAGGGAAAGTCTGACG and EAP-1_{chromo} R TATGCGGCCGCAAGTTCAATAAGCTCTGTTTTGTC and subcloned into pGEX-4T1 between BamHI and NotI. SET-17 full-length cDNA was amplified by PCR from wildtype cDNA using the following primers SET-17 F ATAGAATTCATGAATATTAAACATAATTATATC and SET-17 R TATGCGGCCGCTCACCAAATGAACGGATTCTTGGC and subcloned into pGEX-4T1 between EcoRI and NotI. SET-26_{SET} was amplified by PCR from wildtype cDNA using the following primers SET-26_{SET} F ATAGAATTCGACACGCTGCTCGCCGAGTCGCG and SET-26_{SET} R TATGCGGCCGCCATATGCTCGGCACACTCGAG and subcloned into pGEX-4T1 between EcoRI and NotI. SET-30 full length cDNA was amplified by PCR from wildtype cDNA using the following primers SET-30 F ATAGGATCCATGTCGTCTGGAGATGCTCCGTTA and SET-30 R TATGCGGCCGCCTACATTTCAGCAACAAGTTCT and subcloned into pGEX-4T1 between BamHI and NotI. EAP-1 mutants (F24A, W45A, and Y48A) in the pGEX-4T1 vector were generated by site-directed mutagenesis (Stratagene) using the following sets of primers: F24AF GGAAAGTCTGACGAGATTGCTGAAGTTGAGAAGATTC, F24AR GAATCTTCTCAACTTCAGCAATCTCGTCAGACTTTCC, W45AF GTGCTTCAAGTTCGTGCGTTGGGTTATGGCG, W45AR CGCCATAACCCAACGCACGAACTTGAAGCAC, Y48AF CTTCAAGTTCGTTGGTTGGGTGCAGGCGCCGACGAGGATACCTG, Y48AR CAGGTATCCTCGTCGGCGCCTGCACCCAACCAACGAACTTGAAG. All the fragments generated by PCR were entirely sequenced to verify that there were no mutations introduced by the PCR amplification steps.

RNA interference

E. coli HT115 (DE3) transformed with vectors expressing dsRNA of C28H8.9, C29H12.5, C56G2.1, F10G7.2, F16D3.2, F17A2.3, F53H1.4a, H06O01.2, ZK783.4, T09A5.8, K01G5.2, and T12D8.1 were obtained from the Ahringer library, RNAi to C44B9.4, F22D6.6, F32E10.2, F32E10.5, F32E10.6, K08H2.6, K09A11.5, R06C7.7, T12E12.2, T14G7.1, T23B12.1, Y51H1A.4, Y55B1BR.3, ZK1236.2, and F37A4.8 were from the Open Biosystems library (both a gift from T. K. Blackwell), some RNAi clones were described previously (Greer et al., 2010), and C11G6.3, F26F12.7, F26H11.2a, F26H11.2F, F33E11.6b, H20J04.2, T04D1.4, Y38F2AR.1, Y39B6A.25, Y48G1A.6, Y59A8A.2, ZK973.2, F54F2.2a, F54F2.2b, F10G7.2, F15E6.1, K12H6.11, Y24D9A.2, Y41D4B.12, Y43F11A.5, Y51H4A.12, Y71H2AM.8, Y73B3B.2, Y92H12BR.6, and C15G11.5 were cloned into pL4440 using the primers in Table S3. HT115 bacteria containing the vectors of interest were grown at 37°C and seeded on standard nematode growth medium (NGM) plates containing ampicillin (100 mg ml^{-1}) and isopropylthiogalactoside (IPTG; 0.4 mM).

Whole-mount immunocytochemistry

For whole worm immunostaining, worms were washed several times to remove bacteria and resuspended in fixing solution (160mM KCl, 40 mM NaCl, 20 mM Na_2EGTA, 10 mM spermidine HCl, 30 mM PIPES pH 7.4, 50% methanol, 2% β-mercaptoethanol, 2% formaldehyde) and subjected to two rounds of snap freezing in liquid N_2. The worms were fixed at 4°C for 30 min and washed two times briefly in T buffer (100 mM Tris-HCl pH7.4, 1mM EDTA, 1% Triton X-100) before a 1 hour incubation in T buffer supplemented with 1% β-mercaptoethanol at 37°C. The worms were washed with borate buffer (25 mM H_3BO_3, 12.5 mM

NaOH pH 9.5) and then incubated in borate buffer containing 10 mM DTT for 15 min. Worms were washes with borate buffer and then incubated in borate buffer containing 0.3% H_2O_2. Worms were washed in borate buffer briefly and then were blocked in PBST (PBS pH 7.4, 1% BSA, 0.5% Triton X-100, 5 mM sodium azide, 1 mM EDTA) for 1 hour and then incubated overnight with EAP-1 antibody (1:100 in PBST). Worms were washed 4 times for 25 minutes in PBST and then incubated with Alexa Fluoro 588 secondary antibody (1:50 in PBST). Worms were washed 4 times for 25 minutes in PBST. DAPI (2 mg ml^{-1}) was added to visualize nuclei. The worms were mounted on a microscope slide and visualized using a Zeiss LSM700 confocal system.

Single worm genotyping

Single worms were placed in 5 µl of worm lysis buffer (50 mM KCl, 10 mM Tris pH 8.3, 2.5 mM $MgCl_2$, 0.45% NP40, 0.45% Tween-20, 0.01% gelatin (w/v) and 60 mg ml^{-1} proteinase K), and incubated at -80°C for 1 h, 60°C for 1 h, and then 95°C for 15 min. PCR reactions were performed using the following primers: set-25 F: 5'-CACAATGGATAATAGGGATTTGGG-3', set-25 R: 5'-GGATTTTTCGTTGGTTTTTCGGAC-3', rde-1 F: 5'-TTCATTGAGTTTCCCCACCTACC-3', rde-1 R: 5'-CTCCTCTGTTTTCATTGGCACC-3', set-20 F: 5'-TTTTTTCCCGTTGTGACC-3', set-20 R: 5'-CACCCCAAGTATCCGTTC-3', set-30 F: 5'-CTCCGTTAGAAGTGGTAGGGGTG-3', set-30 R: 5'-GAAGTTGCCTCCAAATGCCG-3', set-32 F: 5'-GCTTCGTCAACACAGTTCAAGAGG-3', set-32 R; 5'-CAGAGCAGGAGAATCCAATACATCTATC-3', set-26 F: 5'-ACCACCACCACCACCACTTG-3', set-26 R: 5'-CTCTTCCTCTTTTGCTTCTTGGC-3', eap-1 F: 5'-TCCATTCAAGTTCCGCAATCC-3', eap-1 R: 5'-CTCTCCATTAGCATCATTCCCG-

3', set-9 F: 5'-CCTGTAAAATCTCTGCGAAAGGG-3', set-9 R: 5'-TGTTGCTGCTGGGAAGCCAC-3', spr-5 F: 5'-AACACGTGCCTCCATGAATATCT-3', spr-5 R: 5'-GAACACGTGTGTTCTCCAGCAA-3', spr-5 I: 5'-CCTATAGAACTTTCCCACAGTG-3', set-13 F: 5'-AAGTTTGGAGGTTGAGAGAGGAGAC-3', set-13 R: 5'-CAGGATGGTGCCGTTTATGTG-3', set-17 F: 5'-ACCATCTTGCTGTGAAACGAGG-3', set-17 R: 5'-TGAACGGATTCTTGGCTGGC-3', jmjd-2 F: 5'-TTTACGCCGCAAAAAAGTGC-3', jmjd-2 R: 5'-TCTACGATGCTCAAGTGGAAGAGTG-3', jmjd-4 F: 5'-TCATCCACAAACCCCGACTCTG-3', jmjd-4 R: 5'-TCAACAGGTATTCCCATCCGAAC-3', psr-1 F: 5'-GTCATTAGGGCGAGATAGATACTCATTAC-3', psr-1 R: 5'-TGGAGCCTAGAGTCTTGTCACGAC-3', jmjd-3.2 F: 5'-TCCAGACAATCAAGTTCCAGCAG-3', jmjd-3.2 R: 5'-GGTTTTTTTCGCTTCTTCCGAC-3', jmjd-3.3 F: 5'-GCTCCACTTATTCTGGTCATTCCC-3', jmjd-3.3 R: 5'-CGTTCCACTTCCTTTCAGCAGC-3', jmjd-1.1 F: 5'-CCGTTAGTGTGTGTAAGATGCTCG-3', jmjd-1.1 R: 5'-CAGACGAGATGGCATTGTTGG-3', jmjd-1.2 F: 5'-TGAGCAACAAGATGGAAGCGG-3', jmjd-1.2 R: 5'-GTGAGAAAACGGCAAAAATGGG-3', . PCR reactions were performed according to the manufacturer's protocol (Invitrogen: Platinum PCR supermix) and PCR reactions were resolved on agarose gels.

Antibodies

The EAP-1 antibody was generated by injection of a fusion protein between GST and full length *C. elegans* EAP-1 and was affinity purified by Covance. EAP-1 antibody was purified against MBP tagged full length EAP-1. The H3K4me2 (07-030), H3K4me3 (07-473), H3K27me1 (07-

448), H3K27me2 (07-452), and H3K27me3 (07-449) antibodies were obtained from Millipore. The Histone H3 (ab1791), H3K9me1 (ab8895), H3K9me3 (ab8898), H3K36me1 (ab9048), H3K36me2 (ab9049), H3K79me1 (ab2886), H3K79me2 (ab3594), and H3K79me3 (ab2621) antibodies were obtained from Abcam. The H3K4me1 antibody (39297) was obtained from Active Motif. The H3K4me1 (CMA302), H3K4me2 (CMA303), H3K9me1 (CMA316), H3K9me2 (CMA317), H3K9me3 (CMA318), and H3K36me3 (13C9) antibodies were a gift from H. Kimura.

Protein analysis by western blot

Worms were grown synchronously to appropriate stages and washed off plates with M9 buffer. Worms were washed several times in M9 buffer and snap frozen in liquid N_2. Sample buffer (2.36% SDS, 9.43% glycerol, 5% β -mercaptoethanol, 0.0945 M Tris-HCl pH 6.8, 0.001% bromophenol blue) was added to worm pellets and they were repeatedly snap frozen in liquid N_2. Worm extracts were sonicated three times for 30 s at 15 W (VirSonic 600) and boiled for 2 minutes before being resolved on SDS–PAGE (15%) and transferred to nitrocellulose membranes. The membranes were incubated with primary antibodies (H3K4me2, 1:2,000; H3, 1:2,000) and the primary antibodies were visualized using horseradish peroxidase-conjugated anti-rabbit secondary antibody (Calbiochem 401393) and ECL Plus (Amersham Biosciences).

Peptide Binding Assay

Streptavidin agarose beads (Millipore 16-126) were washed 3 times in reaction buffer (50 mM Tris-HCl pH 7.5, 150 mM NaCl, 0.2 mM EDTA, 0.1% NP-40). Beads were blocked with 3.5% BSA for 1 hour. Beads were washed 3 times. 1 μg of biotinylated peptide and 10 μg of

bacterially purified GST tagged protein were added and allowed to incubate at 4°C for 2 hours. Beads were washed 5 times with reaction buffer. Samples were eluted in 50 µl of 1x laemmli sample buffer (Laemmli, 1970), boiled, loaded on an SDS-page gel, and Coomassie stained.

Peptide microarray

Methods for peptide synthesis and validation, microarray fabrication, effector protein hybridization and detection, and data analysis were previously described (Rothbart et al., 2012) with the following modification. Each peptide listed in Table S1 was spotted in triplicate eight times per array. Triplicate spots were averaged and treated as a single value for subsequent statistical analysis.

ChIP-Seq

Chromatin preparation was performed as described in (Stock et al., 2007) with some modifications. Strains were maintained at 16°C until the appropriate generation and then shifted to 25°C after birth. 50 µl packed young adult worms were subjected to five freeze/thaw cycles in liquid N_2, and fixed in 1% formaldehyde in PBS (10 min, RT). During fixation, worms were dounced 100 times in a glass homogenizer. Fixation was stopped by addition of Glycine to 0.125M (5 min, RT). Worms were washed in cold PBS, before "swelling" buffer (25 mM HEPES pH 7.9, 1.5 mM $MgCl_2$, 10 mM KCl and 0.1% NP-40) was added to lyse the cells (10 min, 4°C). After resuspension in "sonication" buffer (50 mM HEPES pH 7.9, 140 mM NaCl, 1 mM EDTA, 1% Triton X-100, 0.1% Na-deoxycholate and 0.1% SDS), nuclei were sonicated using a Misonix 3000 (Amplitude 60; 25 cycles; 15s 'on', 45s 'off'; 4°C). The resulting material

was centrifuged twice (10 min, 4°C) at 14,000 rpm. Swelling and sonication buffers were supplemented with 5 mM NaF, 1 mM PMSF, and protease inhibitor cocktail (Roche).

Magnetic beads (Protein G dynabeads, Invitrogen) were washed with sonication buffer before use. Chromatin was immunoprecipitated (overnight, 4°C) with beads and antibody (H3K4me2 Millipore CMA303; H3K9me3 Millipore 07-523; EAP-1). After immunoprecipitation, beads were washed as described previously (Stock et al., 2007). Immune complexes were eluted from beads (65°C, 5 min; and room temperature, 15 min) with 50 mM Tris-HCl pH 8.0, 1 mM EDTA and 1% SDS. Elution was repeated and eluates pooled. Reverse cross-linking was carried out (16h, 65°C) with addition of NaCl and RNase A. EDTA was increased to 5 mM and samples were incubated with 200 μg/ml proteinase K (2h, 50°C). DNA was recovered by phenol-chloroform extraction and ethanol precipitation.

ChIP-seq libraries were prepared using NEBNext DNA library preparation reagents (E6000) and the protocol and reagents concentrations described in the Illumina Multiplex ChIP-seq DNA sample Prep Kit. Libraries were indexed using a single indexed PCR primer. After PCR amplification, 300-600 bp DNA fragments were selected on an agarose gel. Libraries were quantified by Qubit (Invitrogen), and library size was assessed by Bioanalyzer (Agilent). Libraries were sequenced using a HiSeq 2000 (Illumina) to generate 50 bp single end reads. ChIP-seq libraries were generated from two biological repeats for G0 and G20, a single repeat for G10, and four Input samples.

ChIP-seq reads were mapped to the *C.elegans* genome (WS220) using Bowtie and allowing for 0 mismatches, and removing monoclonal reads. Coverage levels within 1 kb windows for EAP-1 and Input samples were normalized by total number of unique perfect alignments for each library and then enrichment was calculated by subtracting the Input from

EAP-1 for each generation. EAP-1 bound regions/genes were defined as those greater than 70% coverage quantile (Table S2). The raw and processed data are deposited at the Gene Expression Omnibus (GEO) under the subseries entry GSE52102. Wildtype whole worm H3K9me3 ChIP-seq data (Gu and Fire, 2010) was downloaded from NCBI (GEO accession number GSE17284) and remapped and analyzed in the same manner.

Worm RNA Extraction and Reverse Transcription Followed by Quantitative PCR

RNA was extracted by addition of 1 ml of Trizol (Invitrogen) for 100µl of worm pellets of young adult worms. Six freeze thaw cycles were performed in liquid nitrogen. The RNA extraction was performed according to the Trizol protocol. The expression of target genes was determined by reverse transcription of 1 µg of total RNA with the Superscript III kit (Invitrogen) followed by quantitative PCR analysis on a Roche Lightcycler 480 II with SYBR Green I Master (Roche) with the following primers: *pan-actin* F: TCGGTATGGGACAGAAGGAC; pan-actin R: CATCCCAGTTGGT GACGATA; asp-17 F: GCGAAGACGTATTGGCAGTT; asp-17 R: TGGAGCATTTGACGGTGTAG; ins-7 F: AGGTCCAGCAGAACCAGAAG; ins-7 R: GAAGTCGTCGGTGCATTCTT; scrm-4 F: TTTTCCTACCGACCTGGATG; scrm-4 R: CCGGACATACGATGAACCTC; ssp-31 F: TTCGCCCAGTCTATGGATTC; ssp-31 R: TTCGGCGTATTGAATGACAA; Y113G7C.1 F: AACGGGACAACTGCGAATAC; Y113G7C.1 R: AGTGTGATCCCGTTGGAGAC. The results were expressed as $2^{(-(\text{Gene of interest number of cycles} - \text{acin number of cycles}))}$. Control PCR reactions were also performed on total RNA that had not been reverse-transcribed to test for the presence of genomic DNA in the RNA preparation.

References:

Andersen, E.C., and Horvitz, H.R. (2007). Two C. elegans histone methyltransferases repress lin-3 EGF transcription to inhibit vulval development. Development (Cambridge, England) *134*, 2991-2999.

Ashe, A., Sapetschnig, A., Weick, E.M., Mitchell, J., Bagijn, M.P., Cording, A.C., Doebley, A.L., Goldstein, L.D., Lehrbach, N.J., Le Pen, J.*, et al.* (2012). piRNAs can trigger a multigenerational epigenetic memory in the germline of C. elegans. Cell *150*, 88-99.

Fritsch, L., Robin, P., Mathieu, J.R., Souidi, M., Hinaux, H., Rougeulle, C., Harel-Bellan, A., Ameyar-Zazoua, M., and Ait-Si-Ali, S. (2010). A subset of the histone H3 lysine 9 methyltransferases Suv39h1, G9a, GLP, and SETDB1 participate in a multimeric complex. Molecular cell *37*, 46-56.

Greer, E.L., Maures, T.J., Hauswirth, A.G., Green, E.M., Leeman, D.S., Maro, G.S., Han, S., Banko, M.R., Gozani, O., and Brunet, A. (2010). Members of the H3K4 trimethylation complex regulate lifespan in a germline-dependent manner in C. elegans. Nature *466*, 383-387.

Grishok, A., Tabara, H., and Mello, C.C. (2000). Genetic requirements for inheritance of RNAi in C. elegans. Science (New York, NY *287*, 2494-2497.

Gu, S.G., and Fire, A. (2010). Partitioning the C. elegans genome by nucleosome modification, occupancy, and positioning. Chromosoma *119*, 73-87.

Hodges, C., and Crabtree, G.R. (2012). Dynamics of inherently bounded histone modification domains. Proceedings of the National Academy of Sciences of the United States of America *109*, 13296-13301.

Katz, D.J., Edwards, T.M., Reinke, V., and Kelly, W.G. (2009). A C. elegans LSD1 demethylase contributes to germline immortality by reprogramming epigenetic memory. Cell *137*, 308-320.

Kleine-Kohlbrecher, D., Christensen, J., Vandamme, J., Abarrategui, I., Bak, M., Tommerup, N., Shi, X., Gozani, O., Rappsilber, J., Salcini, A.E.*, et al.* (2010). A functional link between the histone demethylase PHF8 and the transcription factor ZNF711 in X-linked mental retardation. Molecular cell *38*, 165-178.

Kokura, K., Sun, L., Bedford, M.T., and Fang, J. (2010). Methyl-H3K9-binding protein MPP8 mediates E-cadherin gene silencing and promotes tumour cell motility and invasion. The EMBO journal *29*, 3673-3687.

Laemmli, U.K. (1970). Cleavage of structural proteins during the assembly of the head of bacteriophage T4. Nature *227*, 680-685.

Ni, Z., Ebata, A., Alipanahiramandi, E., and Lee, S.S. (2011). Two SET domain containing genes link epigenetic changes and aging in Caenorhabditis elegans. Aging cell.

Nielsen, P.R., Nietlispach, D., Mott, H.R., Callaghan, J., Bannister, A., Kouzarides, T., Murzin, A.G., Murzina, N.V., and Laue, E.D. (2002). Structure of the HP1 chromodomain bound to histone H3 methylated at lysine 9. Nature *416*, 103-107.

Rothbart, S.B., Krajewski, K., Strahl, B.D., and Fuchs, S.M. (2012). Peptide microarrays to interrogate the "histone code". Methods Enzymol *512*, 107-135.

Stock, J.K., Giadrossi, S., Casanova, M., Brookes, E., Vidal, M., Koseki, H., Brockdorff, N., Fisher, A.G., and Pombo, A. (2007). Ring1-mediated ubiquitination of H2A restrains poised RNA polymerase II at bivalent genes in mouse ES cells. Nat Cell Biol *9*, 1428-1435.

Towbin, B.D., Gonzalez-Aguilera, C., Sack, R., Gaidatzis, D., Kalck, V., Meister, P., Askjaer, P., and Gasser, S.M. (2012). Step-wise methylation of histone H3K9 positions heterochromatin at the nuclear periphery. Cell *150*, 934-947.

Whetstine, J.R., Nottke, A., Lan, F., Huarte, M., Smolikov, S., Chen, Z., Spooner, E., Li, E., Zhang, G., Colaiacovo, M.*, et al.* (2006). Reversal of histone lysine trimethylation by the JMJD2 family of histone demethylases. Cell *125*, 467-481.

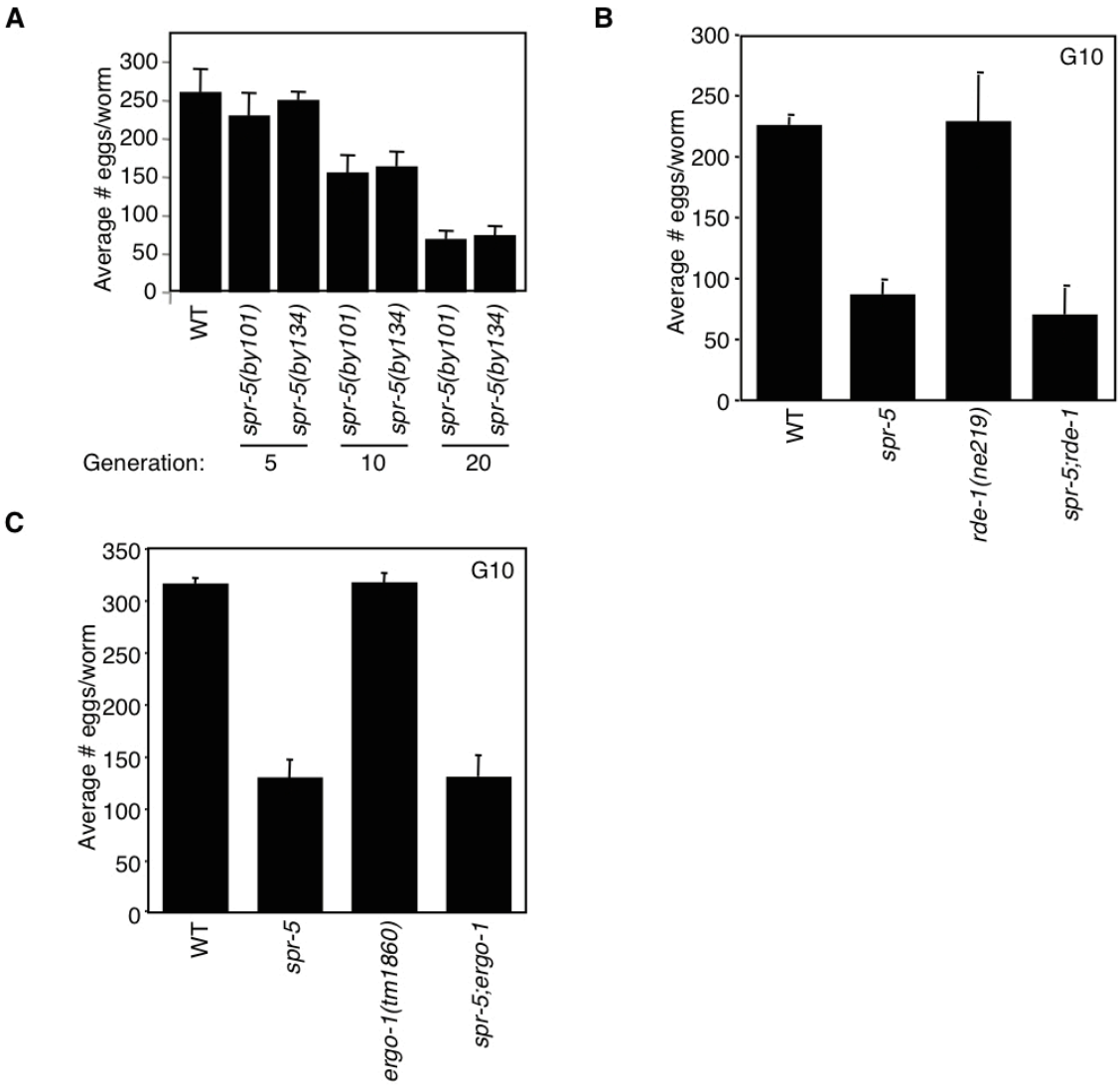

Figure S1: RNAi pathways mediated by *rde-1* and *ergo-1* are not required for inheritance of progressive sterility

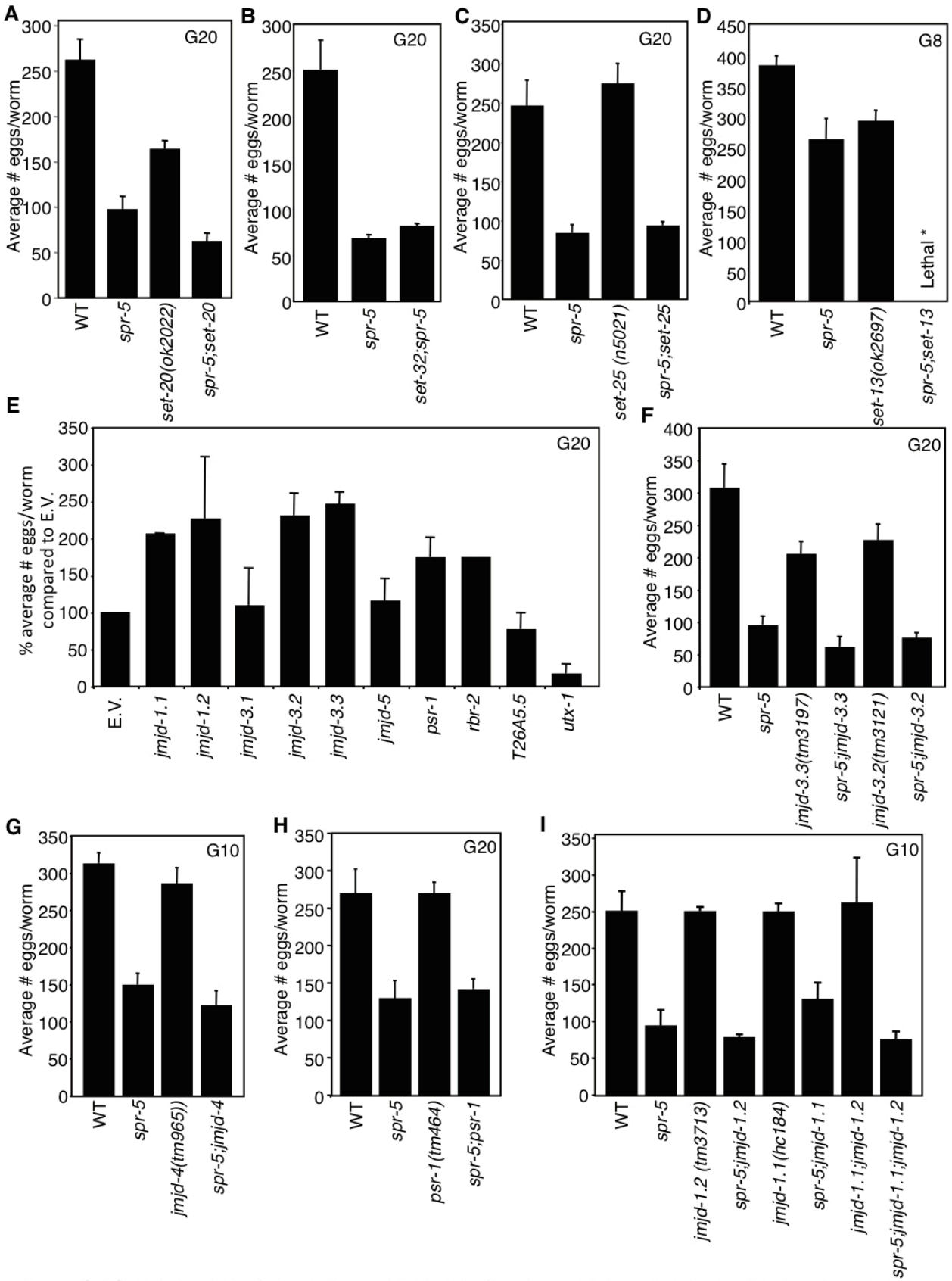

Figure S2: Some methyltransferase and demethylase hits from RNAi screen were not validated by genetic mutants

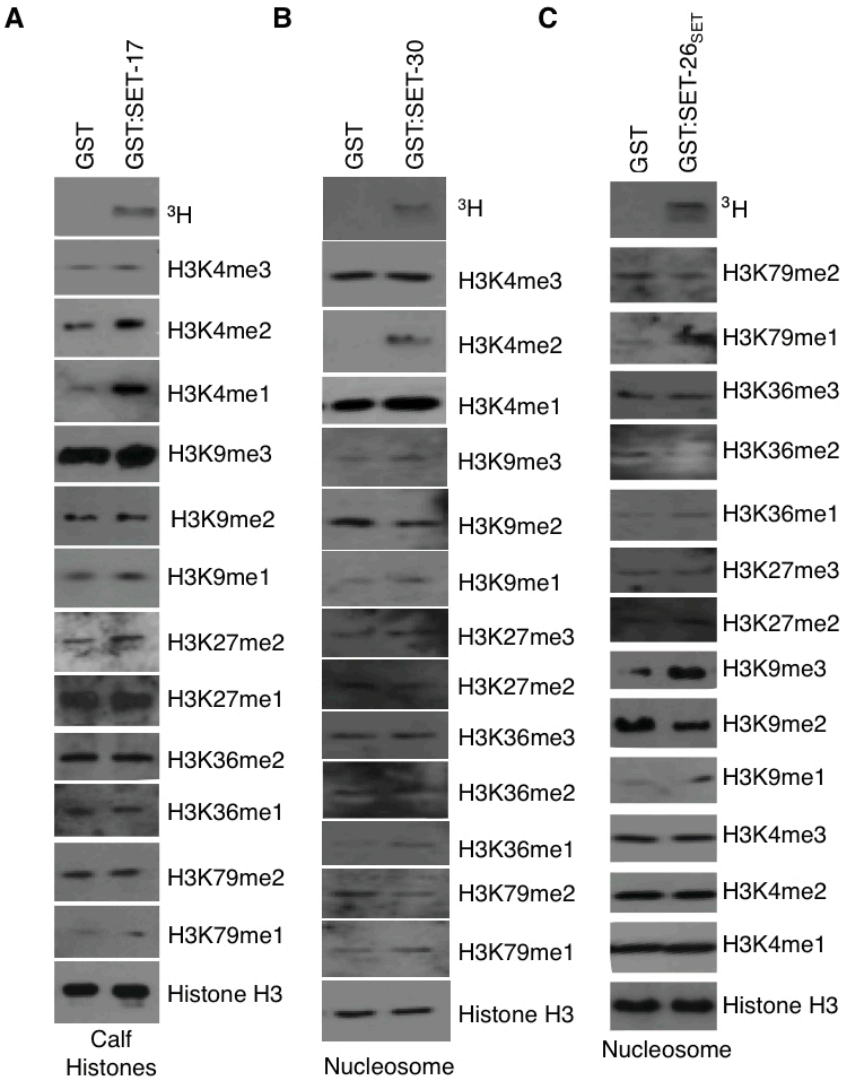

Figure S3: SET-17 and SET-30 are H3K4me1/me2 methyltransferases and SET-26 is an H3K9me3 methyltransferase

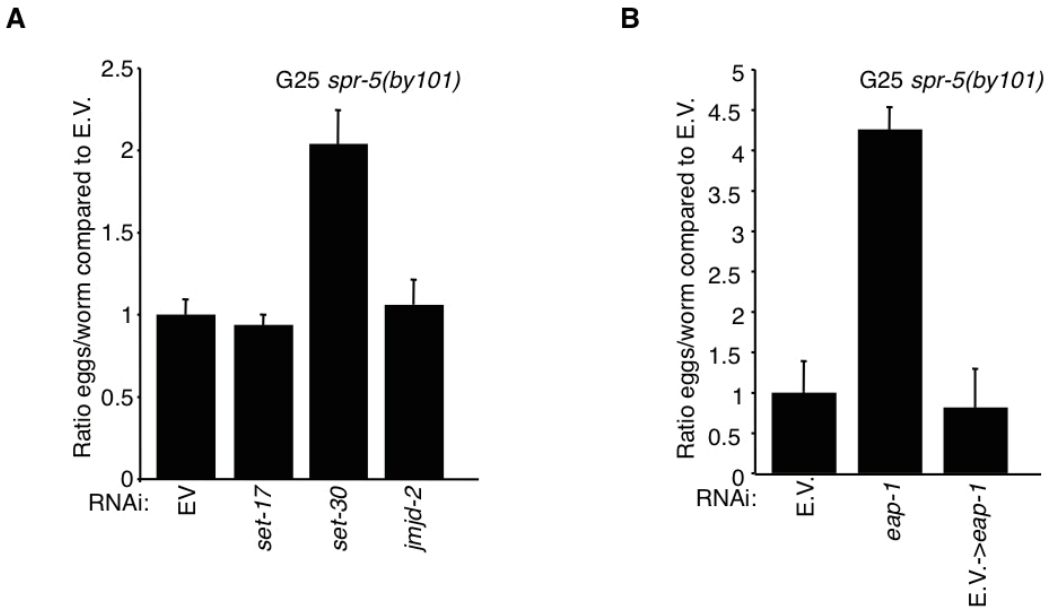

Figure S4: *set-17, jmjd-2,* and *eap-1* RNAi do not revert the progressive sterility of *spr-5(by101)* mutant worms

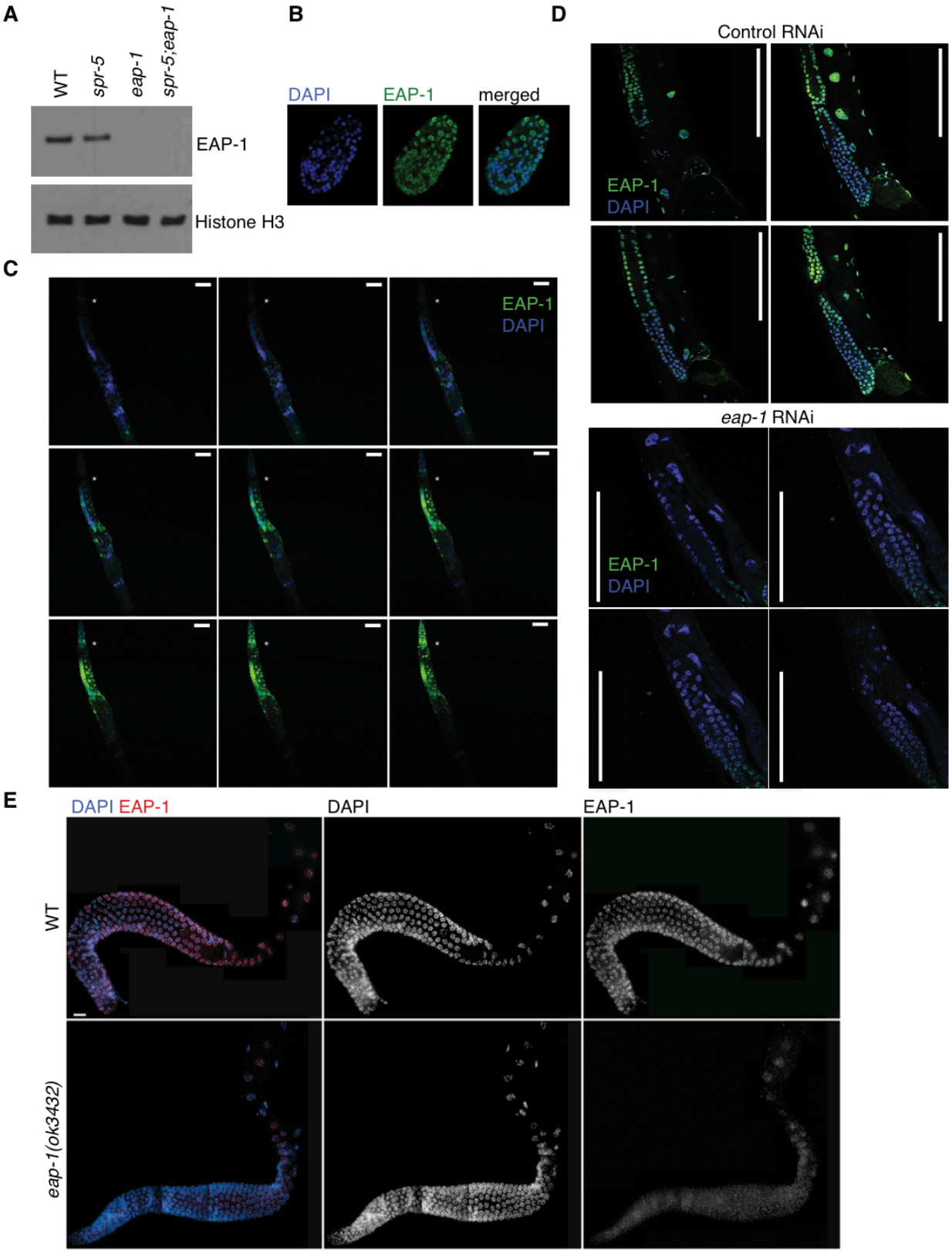

Figure S5: EAP-1 is expressed in every germline nucleus

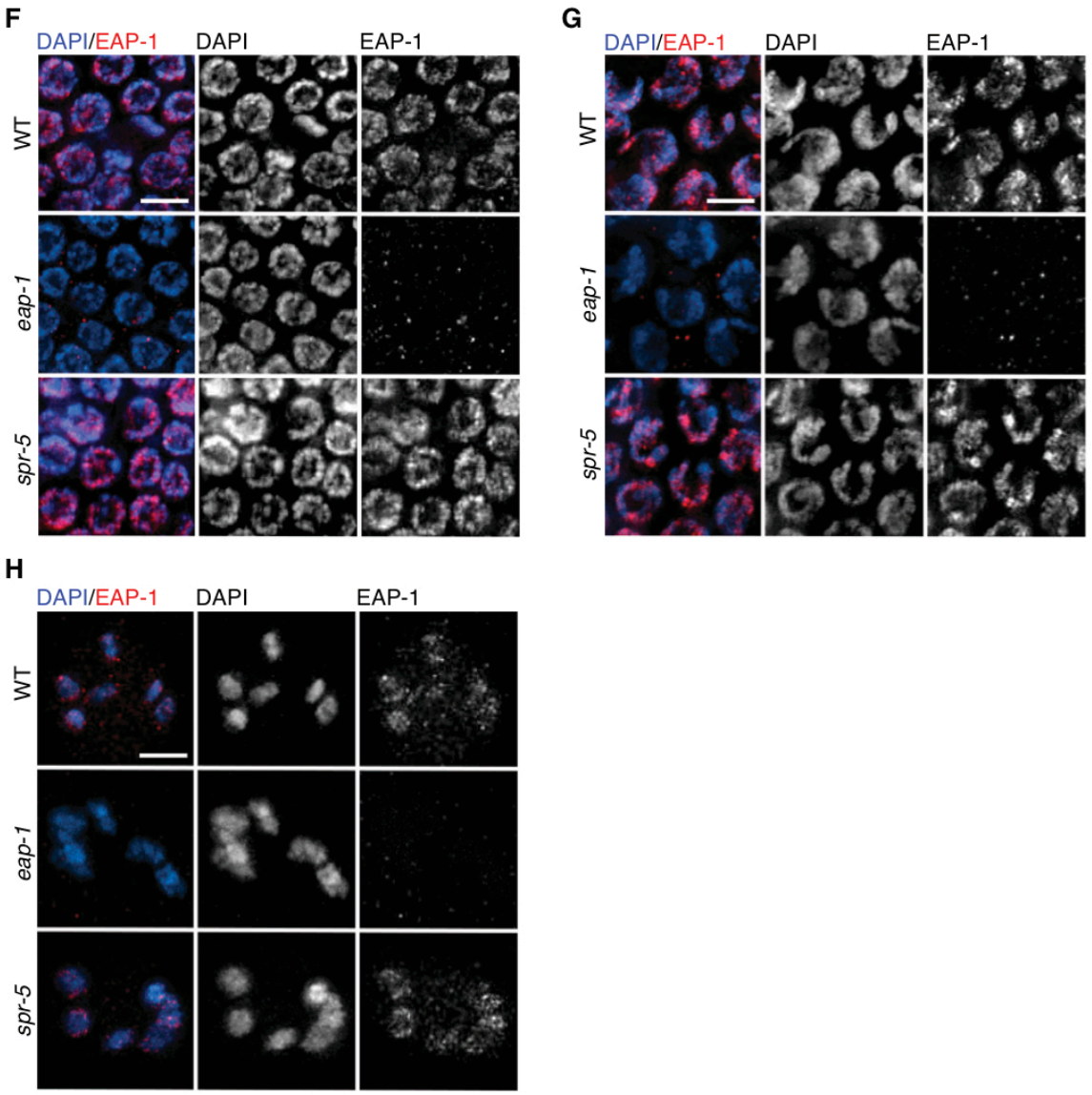

Figure S5: EAP-1 is expressed in every germline nucleus

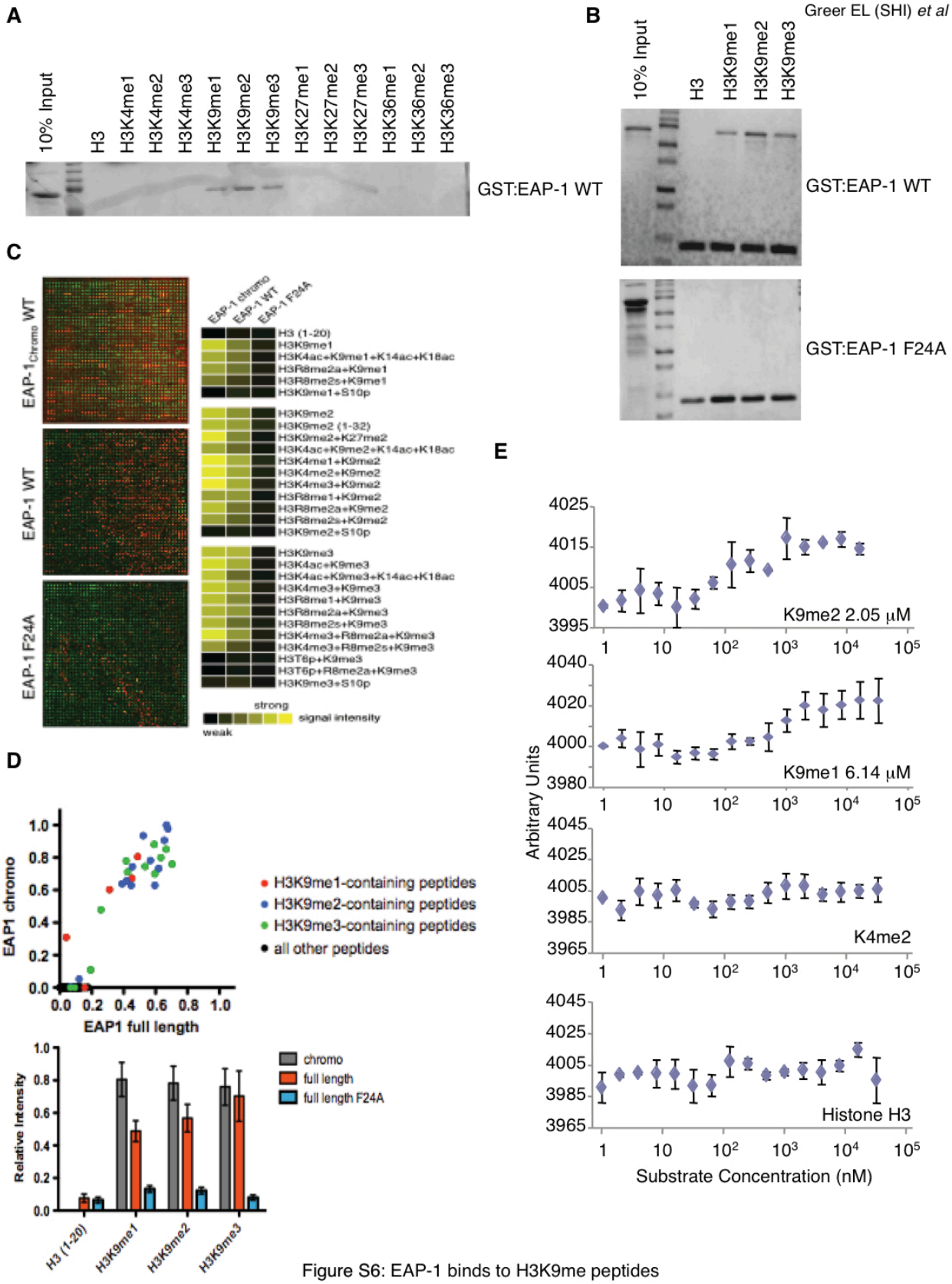

Figure S6: EAP-1 binds to H3K9me peptides

Supplementary Figure Legends

Supplementary Figure 1: RNAi pathways mediated by *rde-1* and *ergo-1* are not required for the inheritance of progressive fertility defects of *spr-5* mutant worms

A) *spr-5(by101)* and *spr-5(by134)* mutant worms display progressive fertility defects (bars represent mean +/- SEM for 3 experiments for wildtype worms, 1 experiment for generation 5, 1 experiment for generation 10, and 2 experiments for generation 20: each experiment consists of average eggs laid for 10 worms of each genotype performed in triplicate). B) *spr-5;rde-1* double mutants lay the same number of eggs as *spr-5(by101)* mutant worms at generation 10. Each bar represents the mean +/- SEM for 3 replicates of 10 worms each. C) *spr-5;ergo-1* double mutants lay the same number of eggs as *spr-5(by101)* mutant worms at generation 10. Graph represents the mean +/- SEM for 2 independent experiments: each experiment consists of average eggs laid for 10 worms of each genotype performed in triplicate.

Supplementary Figure 2: Some methyltransferase and demethylase hits from RNAi screens were not validated by genetic mutants

A) *spr-5;set-20* double mutants lay the same number of eggs as *spr-5(by101)* mutant worms at generation 20. Each bar represents the mean +/- SEM for 3 replicates of 10 worms each. B) *set-32;spr-5* double mutants lay the same number of eggs as *spr-5(by101)* mutant worms at generation 20. Each bar represents the mean +/- SEM for 3 replicates of 10 worms each. C) *spr-5;set-25* double mutants lay the same number of eggs as *spr-5(by101)* mutant worms at generation 20. Each bar represents the mean +/- SEM for 2 independent experiments: each experiment consists of 3 replicates of 10 worms each. D) *spr-5;set-13* double mutants were lethal and therefore *set-13*'s ability to suppress the egg laying defect of *spr-5(by101)* mutant worms

could not be assessed. *set-13(ok2697)* mutant worms layed normal numbers of eggs. E) *spr-5(by101)* mutant worms fed dsRNA of *C. elegans* potential demethylases for 20 generations' effect on egg laying as compared to empty vector RNAi bacteria (E.V.) treated *spr-5(by101)* mutant worms. F) *spr-5;jmjd-3.2* and *spr-5;jmjd-3.3* double mutants lay the same number of eggs as *spr-5(by101)* mutant worms at generation 20. Each bar represents the mean +/- SEM for 3 replicates of 10 worms each. G) *spr-5;jmjd-4* double mutants lay the same number of eggs as *spr-5(by101)* mutant worms at generation 10. Each bar represents the mean +/- SEM for 3 replicates of 10 worms each. H) *spr-5;psr-1* double mutants lay the same number of eggs as *spr-5(by101)* mutant worms at generation 20. Each bar represents the mean +/- SEM for 3 replicates of 10 worms each. I) *spr-5;jmjd-1.1* and *spr-5;jmjd-1.2* double mutants and *spr-5;jmjd-1.1;jmjd-1.2* triple mutants lay the same number of eggs as *spr-5(by101)* mutant worms at generation 10. Graph is a representative experiment where each bar represents the mean +/- SEM for 3 replicates of 10 worms each. *jmjd-1.1(hc184)* deletions effect on egg laying has been tested 3 additional times. *jmjd-1.2(tm3713)* deletions effect on egg laying has been tested 4 additional times.

Supplementary Figure 3: SET-17 and SET-30 are H3K4me1/me2 methyltransferases and SET-26 is an H3K9me3 methyltransferase

A) GST:SET-17 full length protein methylates H3K4me1/me2 as assessed by western blots of *in vitro* methylation assays performed on histones. Histones are purified from calf thymus and are therefore endogenously modified. Radioactive methyltransferase assay is shown on top panel. B) GST:SET-30 full length protein methylates H3K4me1/me2 as assessed by western blots of *in vitro* methylation assay performed on nucleosomes. Nucleosomes are purified from 293T cells

and are therefore endogenously modified. C) GST:SET-26_{SET} methylates histone H3 as detected by ^{3}H incorporation. GST:SET-26_{SET} increases H3K9me3 as assessed by western blots of *in vitro* methyltransferase assays of nucleosomes.

Supplementary Figure 4: *set-17, jmjd-2,* and *eap-1* RNAi do not revert the progressive sterility of *spr-5(by101)* mutant worms

A) *spr-5(by101)* mutant worms fed bacteria expressing dsRNA directed against *set-17* or *jmjd-2* for 5 generations does not revert the egg laying defect of mutant worms fed empty vector control RNAi (E.V.) for 20 generations prior. *set-30* knock down does partially revert the egg laying defect. B) *spr-5(by101)* fed bacteria expressing dsRNA directed against *eap-1* for 5 generations does not revert the egg laying defect of mutant worms fed empty vector control RNAi (E.V.) for 20 generations prior.

Supplementary Figure 5: EAP-1 is expressed in every germline nucleus

A) The EAP-1 antibody is specific and *eap-1(ok3432)* deletion produces a null mutant as predicted and assessed by western blots of whole worm L3 generation 26 lysates. B) EAP-1 is expressed in every cell in wildtype embryos as assessed by whole mount immunofluorescence. C) EAP-1 is expressed in the head region and the germline as assessed by whole mount immunofluorescence. The asterix represents the head of the *C. elegans.* Each panel represents subsequent z stacks of confocal images of *spr-5(by101)* mutant worms stained with EAP-1 and DAPI. Scale bar, 100 μm. D) EAP-1 is expressed in each nuclei of the germline. Z stacks of confocal images from wild type worms treated with either empty vector (control) or *eap-1* RNAi. Each panel represents successive z stacks of confocal images zoomed in on the germline of intact

worms. Scale bar, 100 μm. E) Low magnification images of immunostained whole-mount dissected gonads from either wild type or *eap-1(ok3432)* mutant adult hermaphrodites show EAP-1 expression from the pre-meiotic tip until late pachytene. Scale bar, 10μm. F-H) High magnification images of immunostained whole-mount gonads show EAP-1 expression in every nucleus in the F) premeiotic tip, G) transition zone, and H) diakinesis stages.

Supplementary Figure 6: EAP-1 binds to H3K9 methylated peptides

A) Full length GST tagged EAP-1 binds to H3K9 methylated peptides in *in vitro* binding assays. B) Mutation of F24 to alanine in full length GST tagged EAP-1 eliminates EAP-1's ability to bind to H3K9 methylated peptides. C) GST:EAP-1_{chromo} and GST:EAP-1 full-length bind to only H3K9 methylated peptides on histone peptide microarrays. Mutation of F24 to alanine eliminates this binding activity. EAP-1 binding to H3K9 methylated peptides is inhibited by phosphorylation of serine 10 or threonine 6 on the histone H3 peptides (right panel). D) EAP-1 binds exclusively to H3K9 methylated peptides. Top panel displays every peptide which EAP-1 chromodomain and full length protein binds to on peptide arrays. Bottom panel shows that F24A mutation eliminates EAP-1 binding to H3K9 methylated peptides. E) Microscale thermophoresis of EAP-1_{chromo} and MLA histones shows that EAP-1 has the highest binding affinity for H3K9me3, followed by H3K9me2 and H3K9me1 but shows no binding affinity for H3K4me2 or unmodified histone H3.